

Crystallization of Poly(tetramethylene succinate) in Blends with Poly(ϵ -caprolactone) and Poly(ethylene terephthalate)

K. F. Chong,¹ H. Schmidt,² C. Kummerlöwe,² H. W. Kammer¹

¹School of Chemical Sciences, Universiti Sains Malaysia, 11800 Penang, Malaysia

²University of Applied Sciences Osnabrück, Albrechtstrasse 30, D-49076 Osnabrück, Germany

Received 11 March 2003; accepted 24 September 2003

ABSTRACT: The crystallization behavior of polymer blends of poly(tetramethylene succinate) (PTMS) with poly(ϵ -caprolactone) (PCL) or poly(ethylene terephthalate) (PET) was investigated with differential scanning calorimetry under isothermal and nonisothermal conditions. The blends were prepared by solution casting and precipitation, respectively. The constituent polymers were semicrystalline materials and crystallized nearly independently in the blends. The addition of the second component to PTMS showed that PCL did not significantly influence the crystallinity of the constituents in the blends under isothermal conditions, whereas the crystallization of PTMS was slightly suppressed by crystalline PET. Nonisothermal crystalliza-

tion under constant cooling rates was examined in terms of a quasi-isothermal Avrami approach. In blends, the rates of crystallization were differently influenced by the second component. The rate of the constituent that crystallized at the higher temperature was barely influenced by the second component being in the molten state, whereas the rate of the second component, crystallizing when the first component was already crystalline, was altered differently under isothermal and nonisothermal conditions. © 2004 Wiley Periodicals, Inc. *J Appl Polym Sci* 92: 149–160, 2004

Key words: blends; crystallization; morphology

INTRODUCTION

An important class of polymer systems is formed of blends consisting of two semicrystalline constituents. Complex morphologies may develop in these systems that are strongly influenced by the imposed thermal histories. Blends of poly(tetramethylene succinate) (PTMS) with poly(ϵ -caprolactone) (PCL) or poly(ethylene terephthalate) (PET) belong to this class of systems.

PTMS and PCL are biodegradable aliphatic polyesters. The aromatic polyester PET, however, can induce good mechanical properties, whereas PTMS endows the blends with biodegradability. Usually, the constituents display a high degree of crystallinity. The mechanical properties and rates of biodegradation of the polymers are severely influenced by the morphology and crystallinity. In that respect, blending may help to obtain biodegradable polymers with improved properties. Modified starch was blended with PCL to produce biodegradable packaging materials.^{1,2} Another example is the blending of poly(hydroxy butyrate) with synthetic polymers to improve its mechanical performance.³ Here we study the crystallization behavior and morphology in blends of PTMS with PCL

or PET. In these blends, PTMS crystallizes in different surroundings. In the first type of blend, the liquid–solid transition of PTMS may occur at temperatures at which PCL is in the molten state or its rate of crystallization is extremely low in comparison with that of PTMS. In blends with PET, we have the opposite situation: PTMS crystallizes at temperatures at which PET is in the crystalline state.

The phase behavior, crystallization kinetics, and thermal properties of PCL in miscible binary blends with amorphous components, such as styrene–acrylonitrile copolymer, poly(vinyl methyl ether), poly(vinyl chloride), and chlorinated polyethylene (PE), have been studied extensively in recent years.^{4–9} The influence of the amorphous component on the crystallization behavior of PCL has been found to depend on the interactions between the components and on the glass-transition temperature (T_g) of the blends.

Blends of PTMS with PCL and PET are heterogeneous systems in both the amorphous state and crystalline state. In a system consisting of two crystallizable polymers that form a heterogeneous blend, interactions between the different chain molecules are restricted to the interfacial region between the different phases. We might expect that the crystallization of the component in excess would proceed similarly to that of the pure component. Several studies have revealed, however, that the overall rate of crystallization of the major component can be altered by the presence of a second amorphous component.^{10,11}

Correspondence to: C. Kummerlöwe (c.kummerloewe@fh-osnabrueck.de).

TABLE I
Characteristics of the Polymers

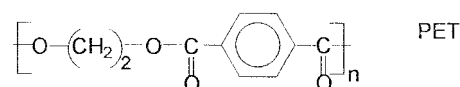
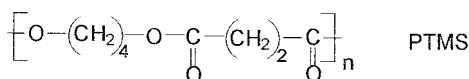
Polymer	M_w (kg/mol)	M_n (kg/mol)	T_m^0 (°C)	T_g (°C)
PTMS	62	34	129	-27
PCL	65	42.5	65	-60
PET	37	19	260	73

There have been only a few studies on the crystal structure and crystallization kinetics of PTMS.^{12,13} This article reports on the crystallization and thermal properties of PTMS in blends with PCL and PET. The aim is to examine the crystallization characteristics of the blends under isothermal and nonisothermal conditions. Also, developing morphologies, grown from the melt, are discussed.

EXPERIMENTAL

Polymers

The applied polymers were commercial. PTMS was supplied by the National Institute of Materials and Chemical Research (Tsukuba, Japan). PCL and PET came from Aldrich and Penfibre, Ltd. (Penang, Malaysia), respectively. The characteristics of the polymers are given in Table I. The chemical structures of these polymers are as follows:



Sample preparation

Blends of PTMS and PCL were prepared via solution casting with 1,2-dichloroethane as a mutual solvent. Stock solutions of the components were used to adjust desired blend compositions. The initial concentration of the blend solutions was 3 wt %. The solvent was evaporated *in vacuo* at about 45°C for more than 1 day. Blends of PTMS and PET were prepared by precipitation. For the preparation of the stock solutions, PTMS and PET were dissolved in a mixture of phenol and dichloroethane (2:3) at a polymer concentration of 0.3 wt %.

Solutions were poured into an excess of methanol, which acted as a nonsolvent, and were precipitated for 1 day. The precipitates were filtered and dried in a

vacuum oven for 2 days to remove the residual solvent. For the neat polymers, the same procedure used for the sample preparation was applied.

Thermal analysis

Differential scanning calorimetry (DSC; TA 3000, Mettler, Giessen, Germany) was used to study the melting and crystallization behavior of the blends by isothermal and nonisothermal crystallization experiments. Details of the experimental procedures for determination of relevant temperatures, melting enthalpy (ΔH_m) and degree of conversion during crystallization [$X(t)$]. The sample weight for all the DSC experiments was approximately 10 mg.

For isothermal crystallization studies, it is convenient to determine the half-time of crystallization ($t_{0.5}$) at the crystallization temperature (T_c). The $t_{0.5}$ values of PTMS in PTMS/PCL blends were determined when PCL was still in the molten state, whereas $t_{0.5}$ of PCL was determined after the isothermal crystallization of PTMS. An analogous procedure was applied for PTMS/PET blends. Here, $t_{0.5}$ of PTMS was determined after the isothermal crystallization of PET. Endotherms obtained after isothermal crystallization for $5t_{0.5}$ were used to study the melting behavior. The heating and cooling rates were fixed at 20°/min for isothermal experiments. Different constant cooling rates (s) were applied for the nonisothermal crystallization experiments (see Table II).

Microscopy

The morphologies of the blends were studied by optical microscopy with a Zeiss polarizing microscope equipped with a Linkam TM 600/s heating/cooling unit (Waterfield/Surrey, UK). PTMS/PCL samples were annealed at 140°C for 10 min. The melt was cooled to 90°C at $s = 20$ K/min, and PTMS crystallization was observed. This was followed by the crystallization of PCL at 40°C. For PTMS/PET blends, an annealing temperature of 270°C was selected, and crystallization was observed at 215 and 90°C, respectively.

RESULTS AND DISCUSSION

Glass transition temperatures

T_g 's were obtained from solution-cast samples and from samples after nonisothermal crystallization at different values of s . T_g 's for PTMS in blends with PCL or PET and T_g 's of PCL in blends with PTMS are shown in Figure 1. T_g of pure PET was 77°C; T_g of PET in PTMS/PET blends was not accessible because it overlapped with the onset of PTMS melting. For PTMS/PCL, there were two T_g 's in the blends, and

TABLE II
Isothermal and Nonisothermal Crystallization Experiments

Step	PTMS/PCL blends	PTMS/PET blends	Extracted data	
			PTMS/PCL	PTMS/PET
Isothermal crystallization				
1	Heating at 20°/min from 25 to 140°C	Heating at 20°/min from 25 to 270°C		
2	Annealing at 140°C for 10 min	Annealing at 270°C for 3 min		
3	Cooling at 20°/min to $T_c^{\text{PTMS}} = 85\text{--}95^\circ\text{C}$ and 102°C	Cooling at 100°/min to $T_c^{\text{PET}} = 211\text{--}217^\circ\text{C}$		
4	Isothermal crystallization of PTMS for $t = 5t_{0.5}$	Isothermal crystallization of PET for $t = 5t_{0.5}$	$t_{0.5}$, $X(t)$ for PTMS	$t_{0.5}$, $X(t)$ for PET
5	Cooling at 20°/min to $T_c^{\text{PCL}} = 37\text{--}44^\circ\text{C}$	Cooling at 100°/min to $T_c^{\text{PTMS}} = 86\text{--}92^\circ\text{C}$		
6	Isothermal crystallization of PCL for $t = 5t_{0.5}$	Isothermal crystallization of PTMS for $t = 5t_{0.5}$	$t_{0.5}$, $X(t)$ for PCL	$t_{0.5}$, $X(t)$ for PTMS
7	Heating at 20°/min from T_c^{PCL} to 140°C	Heating at 20°/min from T_c^{PTMS} to 270°C	T_m , ΔH_m of PCL and PTMS after isothermal crystallization	T_m , ΔH_m of PET and PTMS after isothermal crystallization
Nonisothermal crystallization				
1	Heating at 20°/min from -100 to 160°C	Heating at 20°/min from 25 to 270°C	T_g of solution-cast blends	
2	Annealing at 160°C for 3 min	Annealing at 270°C for 3 min		
3	Cooling to -100°C at $s = 2.5, 5, 7.5, 10, 12.5, 15, 20, 30,$ and $50^\circ/\text{min}$	Cooling to -70° at $s = 5, 10, 15, 20, 25, 30, 35, 40, 45,$ and $50^\circ/\text{min}$	T_{onsr} , $X(T)$ for PTMS and PCL, ΔH_m of PCL and PTMS after nonisothermal crystallization	T_{onsr} , $X(T)$ for PTMS and PET, ΔH_m of PET and PTMS after nonisothermal crystallization
4	Heating at 20 deg/min from -100 to 160°C	Heating at 20 deg/min from -70 to 270°C	T_g , T_m	T_g , T_m

they did not shift in comparison with those of the neat polymers. T_g of PTMS in PTMS/PET blends did not depend on the blend composition. Therefore, it could be inferred that the constituents of the blends were immiscible. The blends were heterogeneous systems in both the amorphous and crystalline states.

Melting behavior

Clearly separated T_c 's and melting temperatures (T_m 's) of the blend constituents of both systems were detected by DSC scans. PCL melting peaks were observed around 60°C; PTMS melted around 120°C, and PET melted around 240°C. Single melting peaks were found for PCL and PET that were independent of the thermal history. PTMS tended to exhibit double melting peaks. Double melting peaks of PTMS were observed for neat PTMS and in blends with PCL and PET when the samples were exposed to isothermal crystallization. Selected endotherms are shown in Figure 2. In the heating scan after nonisothermal crystallization, a cold crystallization peak was detected instead of the lower PTMS melting peak.

Figure 2 shows that the peak temperature of the lower PTMS melting peak increased with increasing T_c , whereas the higher peak temperature slightly de-

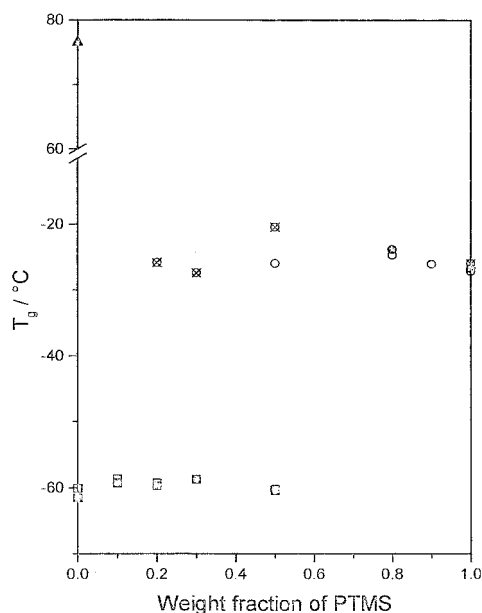


Figure 1 T_g as a function of the PTMS content. For PTMS/PCL blends, the open and solid symbols refer to solution-cast samples and samples after nonisothermal crystallization, respectively: (○,●) PTMS and (□,■) PCL. PTMS/PET blends after quenching at $s = 200^\circ\text{C}/\text{min}$ are also represented: (▲) PET and (⊗) PTMS.

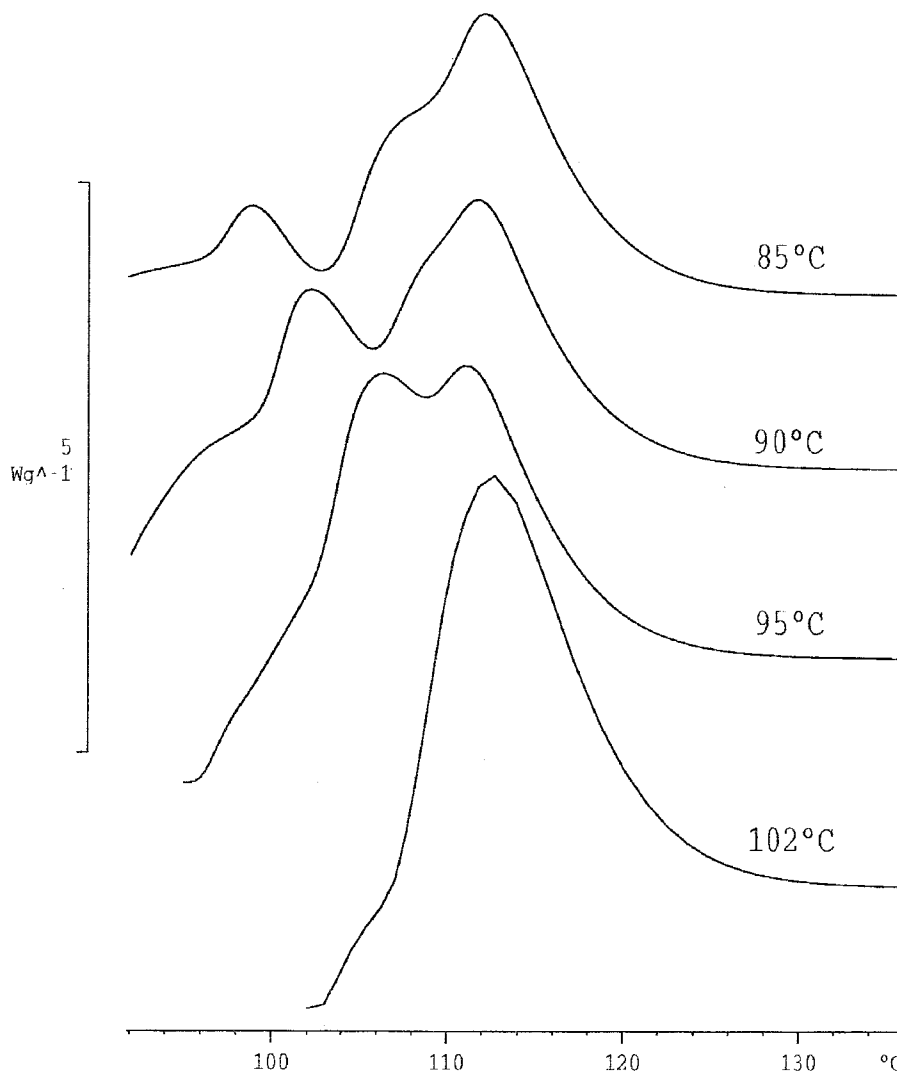


Figure 2 Melting curves of PTMS after isothermal crystallization for a crystallization time of $5t_{0.5}$ and at the indicated T_c values.

creased in the temperature range mentioned. Multiple melting peaks were observed for several other polymers, including poly(3-hydroxybutyrate) (PHB).¹⁴ The peak occurring at the lower temperature was assigned to the melting of the isothermally crystallized material and was frequently used to determine the equilibrium melting temperature (T_m^0). The second peak was the result of the melting of crystals that reorganized during the heating process in the DSC run. The peak temperatures are depicted in Figure 3 as functions of T_c . Figure 2 suggests that at T_c 's above 100°C, a single melting peak could be observed. This was verified by an isothermal experiment at $T_c = 102^\circ\text{C}$. The results are given in Figures 2 and 3.

According to the Hoffman–Weeks equation,¹⁵

$$T_m = \frac{1}{\gamma} T_c + \left(1 - \frac{1}{\gamma}\right) T_m^0 \quad (1)$$

extrapolation to $T_c = T_m$ gives T_m^0 . A detailed inspection of the data presented in Figure 3 for PTMS

shows that the slope ($1/\gamma$) was not constant over the temperature range examined. Such effects were also observed for PCL when the isothermal crystallization was carried out over a large temperature range.¹⁶ Linear regression analysis for data in the T_c range of 86–91°C resulted in $T_m^0 = 129^\circ\text{C}$, which is comparable to the value of 132°C from ref. 13. A considerably higher value, $T_m^0 = 189^\circ\text{C}$, was obtained with the data between $T_c = 91$ and $T_c = 102^\circ\text{C}$ for the calculation of T_m^0 . These results demonstrated that the linearity between T_m and T_c for PTMS was only given in limited temperature ranges. The extrapolation of the linear sections led to rather different apparent T_m^0 values. Therefore, we refer to T_m^0 with respect to the linear range from which it was generated. Furthermore, we note that the slopes of the Hoffman–Weeks plots for the lower and higher temperature ranges were 0.657 and 0.879, respectively. For many other polymers, such as PCL and PHB, a slope of 0.3 was found.^{14,16}

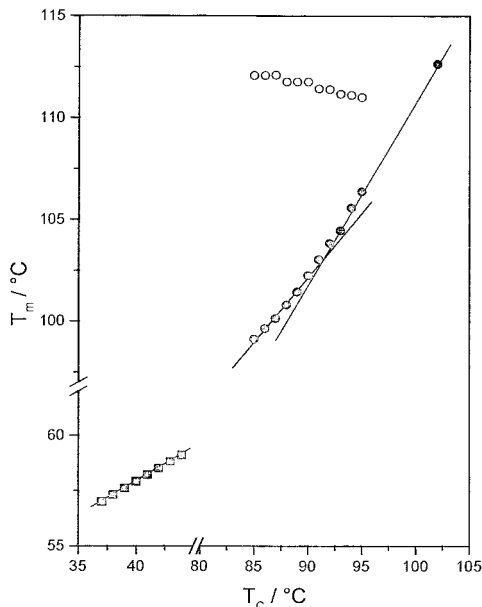


Figure 3 T_m for isothermally crystallized PTMS and PCL as a function of T_c : (●) lower melting peak and (○) higher melting peak PTMS and (■) PCL.

In addition, Figure 3 gives the Hoffman–Weeks plot for PCL with $T_m^0 = 65^\circ\text{C}$ and a slope of 0.3. Data were detected for T_c 's between 37 and 44°C. The values agreed with earlier studies in the same temperature range.¹⁶

In the limits of experimental accuracy, no changes in T_m^0 could be observed as the blend composition of PTMS/PCL blends changed.

In an analogous manner, T_m^0 's of neat PET and blends were determined. Extrapolation resulted in $T_m^0 = 260^\circ\text{C}$ with a slope of 0.29 for pure PET. This result was close to data reported in ref. 17. Also, for PTMS/PET blends, no changes in T_m^0 with the blend composition could be observed.

Crystallinity

We used the melting enthalpies of the constituents, as determined by DSC, to examine the effects of blending on the crystallinity. Figure 4(a) shows the melting enthalpies as a function of the blend composition in solution-cast samples of PTMS and PCL subjected to DSC scanning at 20°C/min. We recognized a high degree of crystallinity for PTMS in the solution-cast samples with a melting enthalpy of 128 J/g. Moreover, the crystallinities of the constituents decreased linearly with the respective concentration. Deviations from linearity occurred neither for PTMS nor for PCL. In miscible blends of PCL with poly(vinyl methyl ether) (PVME), positive deviations of the PCL crystallinity from linearity were observed,^{6,7} and this meant that favorable interactions of the constituents in the

amorphous state did not suppress the crystallization of PCL. Apart from the high degree of PTMS crystallinity, the same tendencies shown in Figure 4(a) were observed for isothermally and nonisothermally crystallized PTMS/PCL samples; no deviations from linearity were detected.

The melting enthalpies of isothermally crystallized PTMS/PET blends as a function of the blend compo-

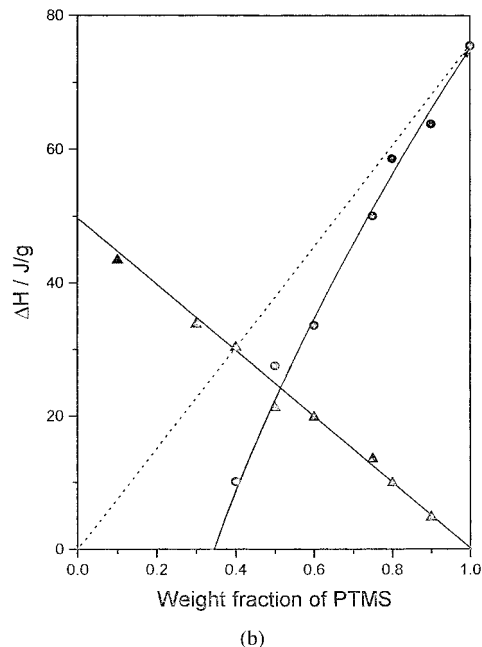
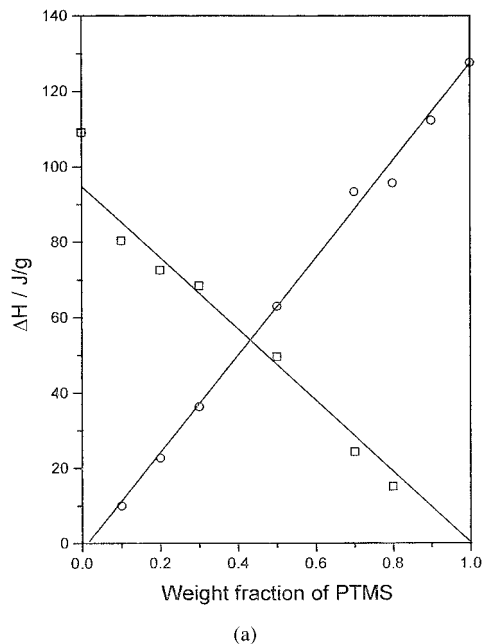


Figure 4 (a) Melting enthalpy (ΔH) as a function of the weight fraction in solution-cast samples of PTMS/PCL blends: (○) PTMS and (□) PCL and (b) ΔH as a function of the weight fraction in PTMS/PET blends after isothermal crystallization for five $t_{0.5}$'s at 90 and 215°C: (●) PTMS ($T_c = 90^\circ\text{C}$) and (▲) PET ($T_c = 215^\circ\text{C}$).



Figure 5 Polarizing optical micrograph of PTMS spherulites grown isothermally at 90°C. The bar corresponds to 50 μm .

sition are depicted in Figure 4(b). The crystallinity of PTMS was markedly lower in samples crystallized from the melt. A melting enthalpy of 75 J/g was detected for PTMS crystallized isothermally at 90°C. The melting enthalpy of PET showed linear behavior over the whole concentration range, whereas the crystallinity of PTMS was markedly depressed with increasing PET concentration. Negative deviations of PTMS crystallinity from linearity occurred already above around 30 wt % PET. Under isothermal conditions, the crystallization tendency of PTMS was noticeably suppressed in heterogeneous blends with PET. The same effect was observed after crystallization under nonisothermal conditions. However, no marked deviations from linearity was detected for the crystallinity of PTMS in solution-cast PTMS/PET samples. Moreover, the crystallinities of PTMS in solution-cast blends with PET agreed to a good approximation with those shown in Figure 4(a) for PTMS blended with PCL.

Morphology and spherulite growth rates

The morphology of the blends and the spherulite growth rate were studied with an optical microscope equipped with a hot stage in samples crystallized from the melt, as described in the Experimental section. The pure polymers PTMS, PCL, and PET formed spherulites if crystallized from the melt. The spherulite sizes were quite different. We observed under the applied experimental conditions spherulites with diameters of approximately 200 μm for pure PTMS (see Fig. 5) and for PTMS in blends with the PTMS matrix.

The spherulite size observed for pure PCL was about 100 μm , but it was drastically reduced to less than 10 μm when PCL crystallized in the presence of the PTMS crystalline phase, even when PCL was the

major component of the blend. PET spherulites were hard to observe with the optical microscope. Their diameters were less than 10 μm in the pure and blended states. In addition, the borderlines of the spherulites were blurred. Therefore, the spherulite growth rate could only be determined for PTMS in the blends under discussion.

PTMS spherulites grown at 90°C are presented in Figure 5. The spherulites exhibited a fibrillar texture. T_g 's revealed that PTMS was immiscible with both PCL and PET (cf. Fig. 1). Therefore, dispersions of the respective minor component developed in the molten blends. In blends with the PTMS matrix, PCL formed small and homogeneous droplets that were quite uniform in size. PTMS spherulites in such a blend are shown in Figure 6. The growing PTMS spherulites incorporated the PCL droplets, and this led to an intraspherulitic distribution of PCL in PTMS. The rejection of molten PCL droplets by the growing PTMS spherulite front into interspherulitic regions could not be observed.

The morphology of a 50/50 PTMS/PCL blend after the crystallization of PTMS at 90°C and after the crystallization of PCL at 40°C is shown in Figure 7. The PTMS spherulites grown at 90°C contained intraspherulitically distributed PCL spots and embraced the PCL melt areas [Fig. 7(a)]. Figure 7(b) shows that in those areas, small PCL spherulites formed at 40°C. In blends with PCL as the major component, the dispersed PTMS islands were larger and unequal in size in comparison with the complementary PCL droplets. Moreover, multiple inclusions occurred; that is, PTMS islands contained small PCL inclusions. As an example, the morphology of a 20/80 PTMS/PCL blend at 90°C is shown in Figure 8.

In the case of PTMS/PET blends with PTMS in excess, PTMS crystallized in the presence of small PET

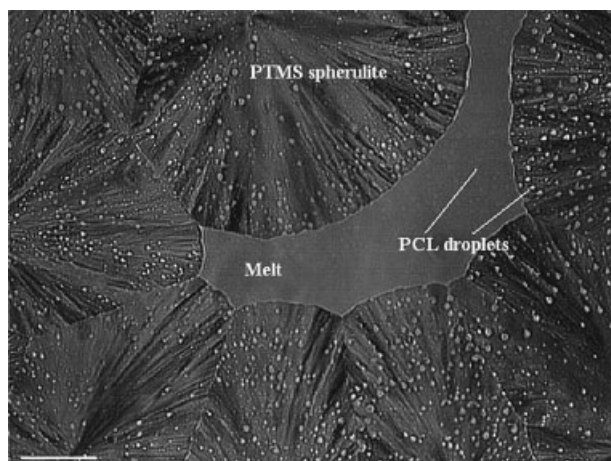
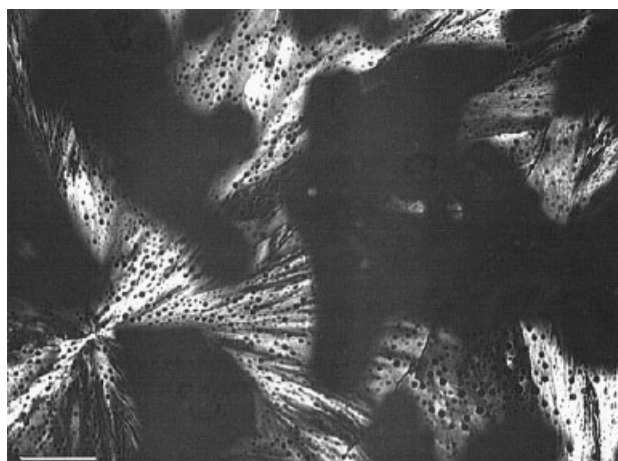
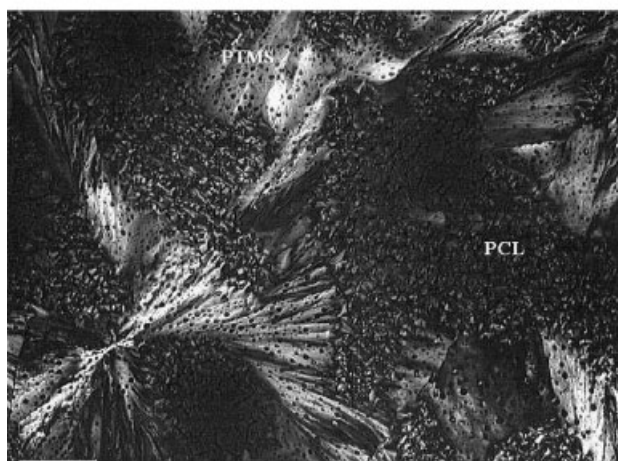


Figure 6 Polarizing optical micrograph of growing PTMS spherulites in an 80/20 PTMS/PCL blend at $T_c = 90^\circ\text{C}$. The bar corresponds to 50 μm .



(a)



(b)

Figure 7 Polarizing optical micrographs of (a) growing PTMS spherulites in a 50/50 PTMS/PCL blend at 90°C and (b) a 50/50 PTMS/PCL blend at 40°C. The bars correspond to 50 μm .

spherulites. The growing PTMS spherulites incorporated these entities, as shown in Figure 9 for an 80/20 PTMS/PET blend after isothermal crystallization at 215 and 90°C.

To reveal more explicitly the influence of the blend composition on the crystallization, we studied the spherulite growth rates of PTMS by optical microscopy. Figure 10 shows growth rates of PTMS spherulites in blends. PTMS spherulites grew slightly faster in the presence of molten PCL than in the presence of crystalline PET. In the range of low PET contents in PTMS/PET blends, the growth rate of PTMS spherulites decreased exponentially with the PET content to a good approximation. At PET contents above around 30 wt %, the rate leveled off. A comparison with Figure 4(b) shows that in blends with PET, both the crystallinity of PTMS and the rate of crystallization were reduced. In blends of PCL and PVME, in which

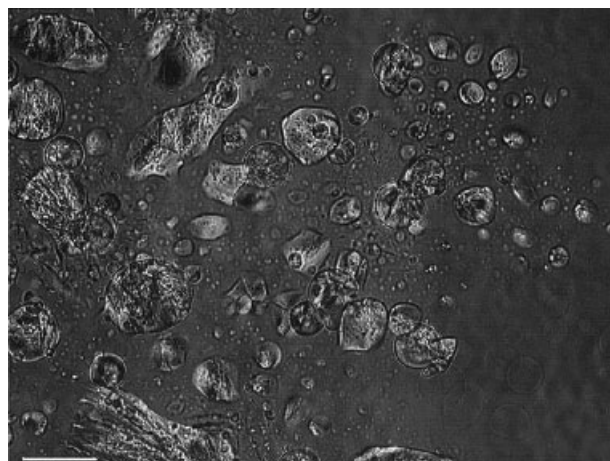


Figure 8 Polarizing optical micrograph of a 20/80 PTMS/PCL blend at 90°C. The bar corresponds to 50 μm .

the constituents were miscible, there was an exponential decrease in the PCL growth rate with increasing PVME content.¹² However, rather than leveling off, the rate was marked by a nonexponential decrease at high PVME contents. In blends with PCL, the growth rate of PTMS slightly increased with increased PCL content.

Kinetics of isothermal crystallization

For the studies of the crystallization kinetics, the polymer blends were exposed to the thermal histories described in the Experimental section. In homogeneous systems, the kinetics of crystallization under isothermal conditions can be adequately discussed in terms of the Avrami equation:¹⁸

$$X(t) = 1 - \exp[-K(T)^{1/n}t]^n \quad (2)$$

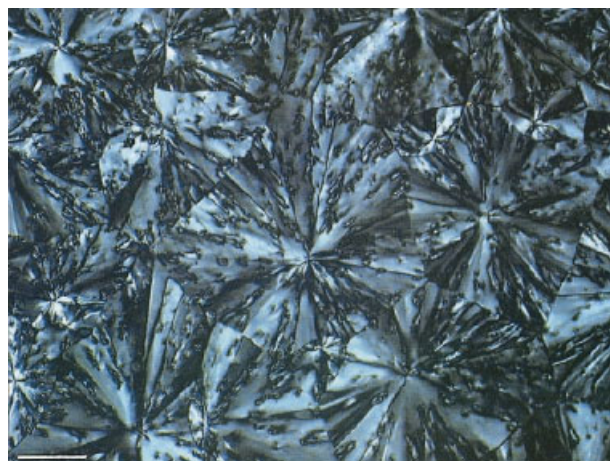


Figure 9 Polarizing optical micrograph of an 80/20 PTMS/PET blend crystallized at $T_c = 215^\circ\text{C}$ and $T_c = 90^\circ\text{C}$. The bar corresponds to 50 μm .

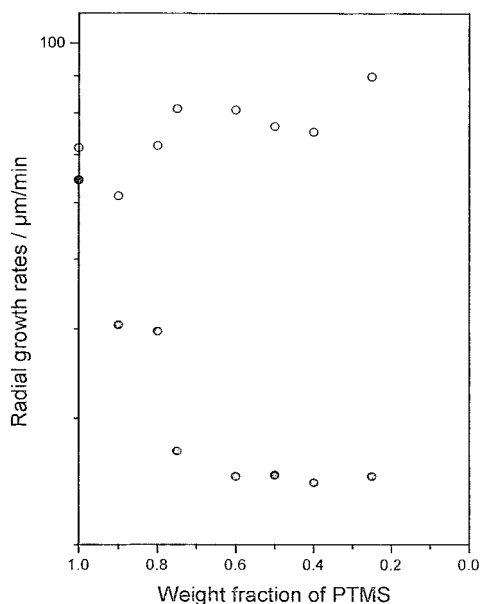


Figure 10 Radial growth rate of PTMS spherulites in blends with (○) PCL and (●) PET under isothermal conditions at 90°C.

where the degree of conversion $[X(t)]$ is defined as ratio of the peak area at time t to the final area $[a(t)/a(\infty)]$. In that way, the conversion is normalized to achieve unity at $t \rightarrow \infty$. $K(T)^{1/n}$ and n represent the overall rate constant and the Avrami exponent, respectively. In addition, we can introduce $t_{0.5}$, defined as the time taken for half of the crystallinity to develop in the isothermal crystallization process. The overall rate constant is closely related to the reciprocal of the half-time of crystallization ($t_{0.5}^{-1}$):

$$t_{0.5}^{-1} = \frac{K^{1/n}}{(\ln 2)^{1/n}} \quad (3)$$

In the heterogeneous systems under discussion, the constituents crystallized independently under isothermal conditions to a good approximation. The component with the higher T_m crystallized at temperatures at which the respective second component did not crystallize but stayed in the molten state, whereas the second component crystallized at temperatures at which the first component was already crystalline. Therefore, the rate of crystallization might have also been influenced by the phase boundaries or morphology of the system. Under these conditions, we had to restrict the application of eq. (2) to the neat components. Results for the pure components could then serve as a reference for the evaluation of the crystallization data of the constituents in the heterogeneous system.

These rate processes, proceeding independently, however, in different surroundings, could be charac-

terized by the corresponding $t_{0.5}$ values. Accordingly, $t_{0.5}^{-1}$ was used as the rate constant of the crystallization process. $t_{0.5}$ was defined independently of eq. (2) and was experimentally accessible. It was estimated from the area of the crystallization peak at the respective value of T_c .

Figure 11 shows $t_{0.5}^{-1}$ versus the reciprocal of undercooling $[(\Delta T)^{-1} = (T_m^0 - T_c)^{-1}]$ for PTMS, PCL, and PET in pure and blended states. We observed for all systems an exponential increase in the rate of crystallization, $(t_{0.5})^{-1}$, with increasing undercooling (ΔT). The rate of crystallization of PTMS did not change markedly in blends with PCL. This situation was in-

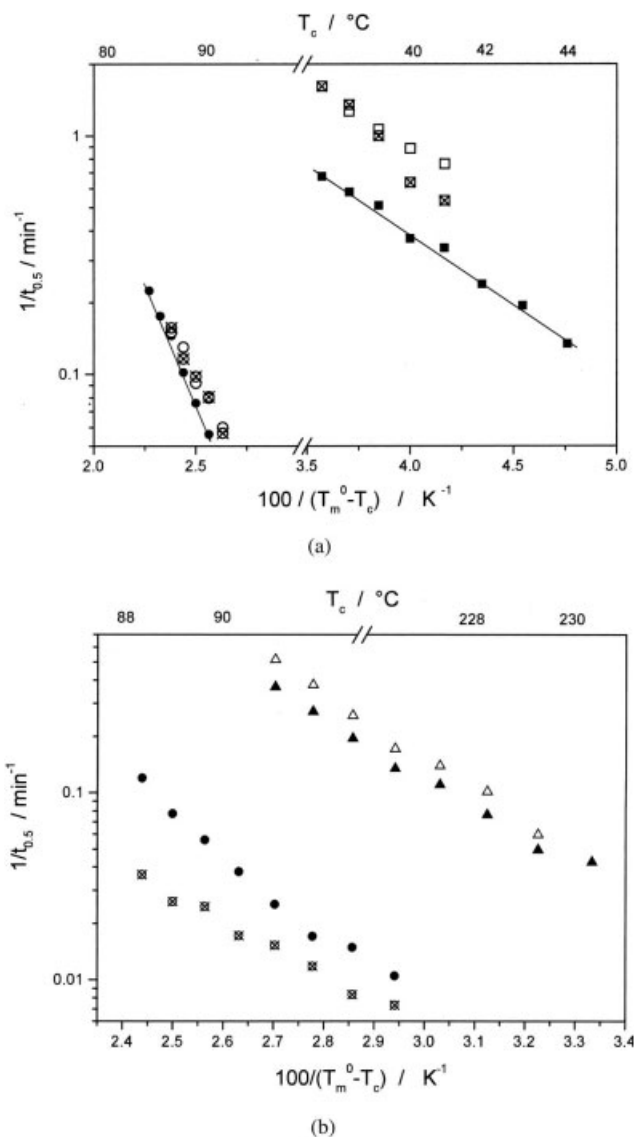


Figure 11 $t_{0.5}^{-1}$ of isothermal crystallization versus $(\Delta T)^{-1}$ for PTMS and PCL in pure and blended states: (a) (●) neat PTMS, (○, ⊗) PTMS in 90/10 and 50/50 PTMS/PCL blends, respectively, (■) neat PCL, and (□, ⊠) PCL in 10/90 and 50/50 PTMS/PCL blends, respectively, and (b) (●) neat PTMS, (⊗) PTMS in a 50/50 PTMS/PET blend, (▲) neat PET, and (△) PET in a 50/50 PTMS/PET blend.

TABLE III
 E_A Values of Isothermal and Nonisothermal Crystallization for Neat Polymers

Polymer	Isothermal		Nonisothermal	
	E_A (kJ mol ⁻¹)	Temperature range (°C)	E_A (kJ mol ⁻¹)	Temperature range (°C)
PTMS	4.0	85–90	2.3	60–82
PCL	1.1	37–42	1.3	16–30
PET	2.9	221–230	0.5	194–220

dependent of the blend composition to a good approximation. This behavior was in qualitative agreement with the results shown in Figure 10. We also recognized that PCL ($T_m^0 = 65^\circ\text{C}$) crystallized more quickly than PTMS, although its ΔT value was less than that of PTMS ($T_m^0 = 129^\circ\text{C}$). The rate of crystallization of PCL increased in blends. This might have been caused by the nucleation activity of crystalline PTMS. A comparison with Figure 4 demonstrates that blending did not alter the degrees of crystallinity of the constituents; however, the rate of PCL crystallization was enhanced in blends, but no systematic variation of the rate with the blend composition was observed.

As mentioned before, molten PCL did not markedly affect the crystallization of PTMS. However, there were different observations on the effect that a molten constituent exerted on the crystallization of a second component in heterogeneous blends. A more pronounced effect was observed in blends of polyamide (PA) and polypropylene (PP).¹¹ Amorphous PP accelerated the rate of PA crystallization. However, previous studies on blends of PP and PE showed the opposite effect on PP crystallization in a certain range of blend compositions.¹⁹ The addition of PE up to 40% PE reduced the rate of PP crystallization. Still higher PE contents caused an increase in the rate.

Figure 11(b) displays the rates of crystallization in PTMS/PET blends. Here PET was the faster crystallizing component at approximately equal ΔT values. For PET, it was the same situation found for PTMS in blends with PCL. The rate of PET crystallization was not markedly influenced by the melt of PTMS. A comparison of Figures 4 and 11(b), however, shows that both the degree of crystallinity of PTMS and the rate of PTMS crystallization were reduced in blends with PET. This result was in qualitative agreement with the dependence of growth rates on the blend composition presented in Figure 10. The activation energy (E_A) of crystallization was obtained from the slopes in Figure 11 as follows:

$$t_{0.5}^{-1} \propto \exp\left(-\frac{E_A}{R \Delta T}\right) \quad (4)$$

where R and ΔT symbolize gas constant and undercooling.

The results are summarized in Table III.

Kinetics of nonisothermal crystallization

There have been several attempts to adequately describe crystallization under nonisothermal conditions. Lorenzo and Silvestre²⁰ recently reviewed the state of the art. We studied nonisothermal crystallization processes with constant values of s . In analogy to eq. (2), one may plot for a constant value of s the conversion $[-\ln(1 - X)]$ versus the time ($\Delta T/s$) at which the temperature difference is the difference between the onset temperature (T_{ons}) and the temperature of interest (T); that is, $\Delta T = T_{\text{ons}} - T$ with $T < T_{\text{ons}}$. The conversion is detected at temperature T . Fixing T_{ons} is important for an adequate evaluation of the process. As it turned out, an adequate choice of T_{ons} was given when T_{ons} was selected in a way that corresponded to a conversion of $X = 0.01$.

Generally, we cannot expect a power law of the type $-\ln(1 - X) \propto (\Delta T/s)^n$ for a constant value of s because the rate constant K of eq. (2) is a function of temperature. However, we can expect quasi-isothermal behavior for a series of nonisotherms, each characterized by a constant value of s , when T is constant:

$$-\ln(1 - X_T) = K(T) \left(\frac{\Delta T}{s}\right)^n \quad \text{for } T = \text{const and } s/\text{const} \quad (5)$$

This means that we can characterize a series of nonisotherms by parameters K and n or, equivalently, with eq. (3), by $t_{0.5}$. Each conversion when T is constant (X_T) refers to a different constant value of s ; that is, each value of X_T refers to a different thermal history of the system. Therefore, eq. (5) characterizes a quasi-isothermal process.

After annealing at 270 and 140°C, respectively, nonisothermal crystallization was carried out with constant values of s between 2.5 and 50 K/min. As under isothermal conditions, the crystallization of the constituents proceeded independently to a good approximation in the blends also under nonisothermal conditions. Figure 12 shows the results of the nonisothermal crystallization of PTMS subjected to different

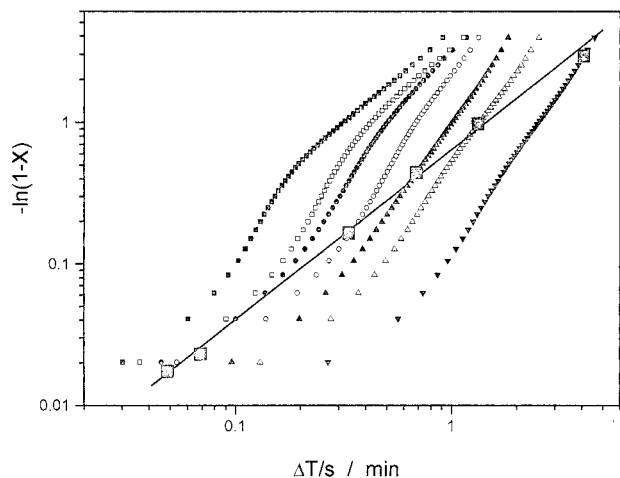


Figure 12 Results of the nonisothermal crystallization of PTMS with different constant values of s : 2.5, 5, 7.5, 12.5, 20, 30, and 50 K/min (from right to left). The solid squares refer to $T = 78^\circ\text{C}$.

values of s . For $s \rightarrow 0$, the nonisotherms approached Avrami-like behavior. With increasing s , deviations from the power law, equivalent to eq. (2), became more pronounced. As Figure 12 demonstrates, data points for a constant value of T obeyed eq. (5) to a very good approximation. This justified characterizing the kinetics of crystallization at different constant values of s by $[t_{0.5}(T)]^{-1}$, as for isothermal crystallization. For the determination of $t_{0.5}$ at selected temperatures with eq. (5) only, sets of experimental data were used that consisted of more than three data points with a correlation coefficient greater than 0.99.

We note here that the example for $T = 78^\circ\text{C}$, given in Figure 12, showed that nonisotherms with sufficiently high s values did not contribute to eq. (5). A reduction of the temperature shifted the straight line upward. This meant that nonisotherms belonging to sufficiently low s values did not contribute to the power law of eq. (5). We recognize that for each constant value of T , only nonisotherms in a limited range of s (which is constant) are included in the quasi-isothermal approach of eq. (5). The conclusion is that for sufficiently high temperatures, the rate constant is dominantly ruled by nonisotherms that are in close proximity to isothermal conditions, whereas quasi-isothermal rates at low temperatures are governed by nonisotherms with high values of s .

An analysis of the experimental data in terms of eq. (5) led to exponents n quite close to unity for the polymers under discussion. This means that the nonisothermal crystallization process might be seen approximately as a first-order rate process.

Figure 13 shows $t_{0.5}^{-1}$, from eq. (5), versus the reciprocal of the temperature difference, $(T_m^0 - T)^{-1}$, for the neat polymers. For comparison, $t_{0.5}^{-1}$ values of isothermal crystallization are indicated. We recognize that for

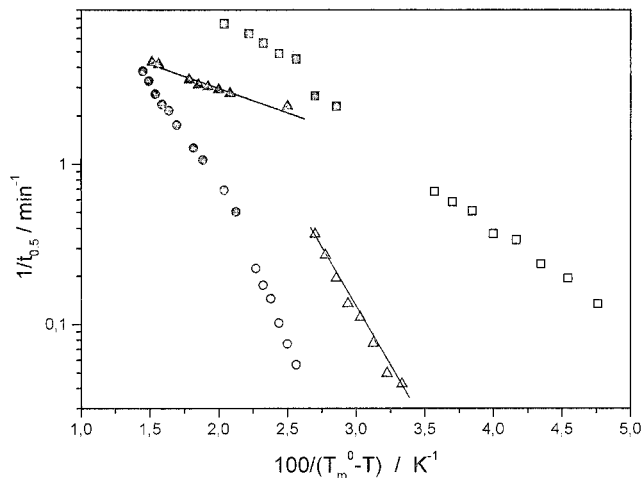


Figure 13 $t_{0.5}^{-1}$ versus $(\Delta T)^{-1}$ for the neat polymers under nonisothermal conditions (solid symbols) and isothermal conditions (open symbols): (●,○) PTMS, (▲,△) PET, and (■,□) PCL.

a certain range of temperatures, at a constant value of ΔT , PCL exhibited the highest crystallization rate and PTMS exhibited the lowest. Moreover, the E_A values of crystallization characterizing the isothermal process exceeded those of the nonisothermal process. Data determined with eq. (4) are summarized in Table III. As a result, we observed a merging of the rate constants belonging to the quasi-isothermal and isothermal process at a sufficiently high temperature (T_{merging}). At temperatures less than T_{merging} , the quasi-isothermal approach led to lower rates than the isothermal process. This behavior was consistent with the previous discussion. At low temperatures, only nonisotherms contributed to the quasi-isothermal ap-

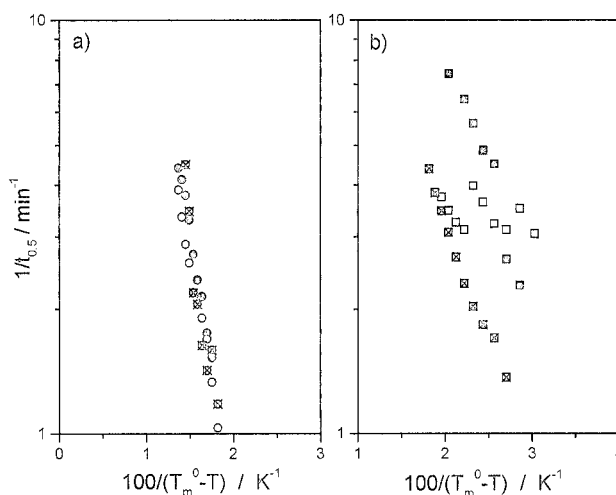


Figure 14 $t_{0.5}^{-1}$ versus $(\Delta T)^{-1}$ for PTMS and PCL in selected PTMS/PCL blends crystallized nonisothermally: (a) PTMS in (●) 100/0, (○) 90/10, and (⊗) 50/50 blends and (b) PCL in (■) 0/100, (□) 10/90, and (⊠) 80/20 blends.

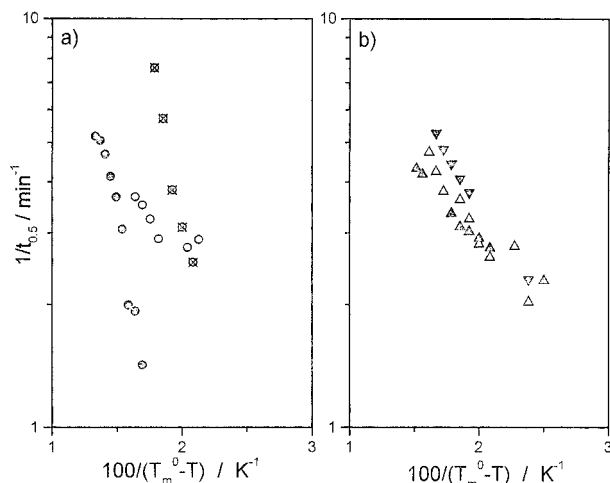


Figure 15 $t_{0.5}^{-1}$ versus $(\Delta T)^{-1}$ for PET and PTMS in PTMS/PET blends crystallized nonisothermally: (a) PTMS in (●) 100/0, (○) 90/10, and (⊗) 50/50 blends and (b) PET in (▲) 0/100, (△) 10/90, and (▼) 50/50 blends.

proach, which belonged to sufficiently high values of s . Therefore, the change of conversion from one value of s to another at a constant value of T was small, leading to crystallization rates lower than those found under isothermal conditions. At $T \approx T_{\text{merging}}$, nonisotherms with low values of s contributed dominantly to the quasi-isothermal process, and rate constants of the nonisothermal process smoothly approached those of the isothermal process.

The crystallization behavior under nonisothermal conditions for the constituents in blends is shown in Figures 14 and 15. We recognize that the components that crystallized when the respective second component was in the molten state behaved similarly in the blended and neat states. Neither the rate constant of PTMS nor that of PET changed markedly in blends with PCL or PTMS, respectively, in comparison with the pure state. A comparison with Figures 11(a,b) reveals that this behavior was in rather good agreement with the results for isothermal crystallization. For the respective second component, crystallizing when the first component was already crystalline, the situation became more complex because of the development of complex morphologies, as Figures 7 and 8 demonstrate. As a result, we observed a more pronounced scatter of data than for the neat polymers. Moreover, a distinct dependence of the rate constant at a constant value of ΔT on the blend composition could not be observed. Qualitatively, we found that for blends with the crystallizing component in excess, increasing the rate of PTMS crystallization pointed toward the nucleating activity of crystalline PET in the blends under nonisothermal conditions, whereas crystalline PTMS reduced the rate of crystallization of PCL over a wide range of temperatures. At sufficiently high temperatures, we can state an approach of the

PCL rate toward that of pure material. This behavior of both PCL and PTMS in blends under nonisothermal conditions was in contrast to results plotted in Figures 10 and 11 for isothermal conditions.

CONCLUSIONS

We demonstrated that PTMS was immiscible with PCL and PET in the amorphous and crystalline states. In PTMS, spherulites grew with a fibrillar texture. Dispersions of the minor component developed in solution-cast blends of PTMS with PCL and PET. Fine and nearly homogeneous dispersions of PCL or PET were observed in blends with PTMS in excess, whereas more coarse-grained and less homogeneous structures occurred in the opposite case. Moreover, multiple inclusions of PCL in PTMS islands were seen when PTMS was the minor component and formed the dispersed phase.

The crystallization behavior of the polymers and blends was investigated extensively. The results showed that crystallinities of the constituents after isothermal and nonisothermal crystallization were not significantly altered in PTMS/PCL blends. In blends with PET, however, crystalline PET suppressed the crystallization of PTMS. The constituents crystallized in sufficiently distinct temperature ranges. PET crystallized when PTMS was in the molten state and was unable to do so, and the same was true for the crystallization of PTMS and PCL. As a result, we can say that the constituents crystallized in blends independently over the course of time to a good approximation. In heterogeneous systems, morphological features could influence the rate constant determined with the Avrami approach. Therefore, $t_{0.5}^{-1}$ values were used as rate constants.

The crystallization kinetics were studied under isothermal and nonisothermal conditions. The latter were discussed in terms of a quasi-isothermal approximation. This approach was applied successfully under nonisothermal conditions with a constant value of s . The rate constants under isothermal conditions displayed a stronger temperature dependence than the rate constants characterizing the nonisothermal process. Therefore, the rates of crystallization of the quasi-isothermal process and under isothermal conditions were approached at the limit of low ΔT values or at T_{merging} . For $T < T_{\text{merging}}$, the former rates were lower than those of isothermal crystallization.

In blends, the rate of crystallization for the component crystallizing at the higher temperature, at which the respective second component was still in the melt, did not change markedly in blends under isothermal or nonisothermal conditions. For PTMS, the growth rate of spherulites was reduced with an increasing content of crystalline PET under isothermal conditions. Eventually, it leveled off at a PET content of

about 30–40 wt %. Under nonisothermal conditions, however, the addition of PET caused an increasing rate of PTMS crystallization. Different behaviors under isothermal and nonisothermal conditions were also displayed by PCL in blends with PTMS. In the former case, its rate of crystallization was enhanced when crystalline PTMS was present, whereas under nonisothermal conditions it was reduced over a certain range of temperatures, and almost no influence of crystalline PTMS was observed at sufficiently high temperatures.

References

1. Pranamuda, H.; Toikiwa, Y.; Tanaka, H. *J Environ Polym Degrad* 1996, 4, 1.
2. Odusanya, O. S.; Ishiaku, U. S.; Azemi, B. M. N.; Manan, B. D. M.; Kammer, H. W. *Polym Eng Sci* 2000, 40, 1298.
3. Avella, M.; Martuscelli, E.; Greco, P. *Polymer* 1991, 32, 1647.
4. Schoene, K.; Kressler, J.; Kammer, H. W. *Polymer* 1993, 34, 3704.
5. Kammer, H. W.; Kummerlöwe, C. *Adv Polym Blends Alloys Tech* 1994, 5, 132.
6. Oudhuis, A. A. C. M.; Thiewes, H. J.; vanHutten, P. F.; ten-Brinke, G. *Polymer* 1994, 35, 3936.
7. Yam, W. Y.; Ismail, J.; Kammer, H. W.; Schmidt, H.; Kummerlöwe, C. *Polymer* 1999, 40, 5545.
8. Koleske, J. V.; Lundberg, R. D. *J Polym Sci Part A-2: Polym Phys* 1969, 7, 795.
9. Defieuw, G.; Groeninckx, G.; Reynaers, H. *Polymer* 1989, 30, 595.
10. Campoy, I.; Arribas, J. M.; Zaporta, M. A. M.; Marco, C.; Gomez, M. A.; Fatou, J. G. *Eur Polym J* 1995, 31, 475.
11. Piglowski, J.; Gancarz, I.; Wlazlak, M.; Kammer, H. W. *Polymer* 2000, 41, 6813.
12. Ihn, K. J.; Yoo, E. S.; Im, S. S. *Macromolecules* 1995, 28, 2460.
13. Miyata, T.; Masuko, T. *Polymer* 1998, 39, 1399.
14. Dubini Paglia, E.; Beltrame, P. L.; Canetti, M.; Serves, A.; Marcandalli, B.; Martuscelli, E. *Polymer* 1993, 34, 996.
15. Hoffman, J. D.; Weeks, J. *J Res Natl Bur Stand Sect A* 1962, 66, 13.
16. Kummerlöwe, C.; Morgenstern, U.; Kammer, H. W.; Keul, H.; Höcker, H. *Polym Networks Blends* 1993, 3, 137.
17. Yoshikai, K.; Nakayama, K.; Kyotani, M. *J Appl Polym Sci* 1996, 62, 1331.
18. Mandelkern, L. *Crystallization of Polymers*; McGraw-Hill: New York, 1964.
19. Martuscelli, E.; Pracella, M.; Avella, M.; Greco, R.; Rastoga, G. *Makromol Chem* 1980, 181, 957.
20. Di Lorenzo, M. L.; Silvestre, C. *Prog Polym Sci* 1999, 24, 917.